Reactions of Copper(II) Salts with 3{5}-*tert*-Butylpyrazole: Double-Cubane Complexes with Bound Exogenous Anions, and a Novel Pyrazole Coordination Mode

Xiaoming Liu,[a] Judith A. McAllister,[b, c] Marcelo P. de Miranda,[a] Eric J. L. McInnes,[d] Colin A. Kilner,[a] and Malcolm A. Halcrow*[a]

Abstract: Reaction of CuX_2 (X^-=Cl^-, Br^-, NO_3^-), NaOH, and 3{5}-*tert*-butylpyrazole (Hpz^{tBu}) in a 1:1:2 molar ratio in MeOH at 293 K for three days affords $[\{Cu_3(Hpz^{tBu})_6(\mu_3\text{-}X)(\mu_3\text{-}OH)_3\}_2Cu]X_6$ (X^-=Cl^-, **1**; X^-=Br^-, **2**; X^-=NO_3^-, **3**) in moderate yields. These compounds contain a centrosymmetric, vertex-sharing double-cubane $[\{Cu_3(Hpz^{tBu})_6(\mu_3\text{-}X)(\mu_3\text{-}OH)_3\}_2Cu]^{6+}$ core, surrounded by a belt of six hydrogen-bonded X^- ions. For **1** and **2**, the ring of guest anions has near C_3 symmetry, that is slightly distorted owing to the axis of Jahn–Teller elongation at the central Cu ion. For **3** only, the NO_3^- guest ions are crystallographically disordered, reflecting their poor complimentarity with complex host. A similar reaction employing CuF_2 yields $[\{Cu_3(Hpz^{tBu})_4(\mu\text{-}pz^{tBu})_2(\mu\text{-}F)_2(\mu_3\text{-}F)\}_2]F_2$ (**4**), whose structure contains a cyclic hexacopper core with approximate C_{2v} symmetry. Finally, an analogous reaction using $Cu(NCS)_2$ gives a mixture of *trans*-$[Cu(NCS)_2(Hpz^{tBu})_2]$ (**5**) and $[Cu_2(NCS)_2(\mu\text{-}pz^{tBu})_2(\mu\text{-}Hpz^{tBu})(Hpz^{tBu})_2]$ (**6**). The latter compound contains a Hpz^{tBu} ligand bridging the two Cu ions in an unusual κ^1,μ-coordination mode. The variable temperature magnetic properties of **1**–**3** show antiferromagnetic behavior, leading to a $S=\frac{1}{2}$ ground state in which the seven copper(II) ions are associated into three mutually independent distinct spin systems. In confirmation of this interpretation, *Q*-band EPR spectra of solid **1** and **2** at 5 K also demonstrate a $S=\frac{1}{2}$ spin system and exhibit hyperfine coupling to three $^{63,65}Cu$ nuclei. Unusually, the coupling is manifest as an eight-line splitting of the parallel feature, rather than the usual 10 lines. This has been rationalized by a spin-projection calculation, and results from the relative magnitudes of coupling to the three Cu nuclei. UV/Vis and mass spectrometric data show that **1**–**4** decompose to lower nuclearity species in solution.

Keywords: cluster compounds · copper · hydrogen bonds · N ligands

Introduction

There are several, disparate examples of polymetallic clusters or aggregates containing encapsulated guest molecules or ions. This phenomenon is especially prevalent in polyoxometallate chemistry, where there are direct bonds between the encapsulated guest, which is usually an oxoanion, and metal ions in the metallate cage.[1] However, there are also an increasing number of polynuclear coordination compounds, with two- or three-dimensional cage structures surrounding a guest species.[2] In these latter compounds there are often no covalent bonds between the guest and the complex host; instead, the guest interacts with the cage only by electrostatics, hydrogen-bonding, or other secondary interactions. The metal/ligand system in these compounds has often been designed to afford polynuclear products,[2] so it can be uncertain whether formation of the cage structures is templated by the guest anion; or, whether the guest simply occupies a cavity within a preformed cage upon crystallization.

[a] Dr. X. Liu, Dr. M. P. de Miranda, C. A. Kilner, Dr. M. A. Halcrow
School of Chemistry, University of Leeds
Leeds LS2 9JT (UK)
Fax: (+44) 113-343-6565
E-mail: M.A.Halcrow@chem.leeds.ac.uk

[b] Dr. J. A. McAllister
Department of Chemistry, University of Cambridge Lensfield Road,
Cambridge CB2 1EW (UK)

[c] Dr. J. A. McAllister
Interdisciplinary Research Centre in Superconductivity University of Cambridge
Madingley Road, Cambridge CB3 0HE (UK)

[d] Dr. E. J. L. McInnes
EPSRC CW EPR Service, Department of Chemistry
University of Manchester
Oxford Road, Manchester M13 9PL (UK)

 DOI: 10.1002/chem.200305613

There are only a small number of examples where genuine anion templating of a cage structure through noncovalent interactions has been demonstrated.[3–6]

We have recently reported the crystal structure and magnetic properties of $[\{Cu_3(Hpz^{tBu})_6(\mu_3\text{-}Cl)(\mu_3\text{-}OH)_3\}_2Cu]Cl_6$ (**1**; Hpz^{tBu} = 5-*tert*-butylpyrazole), which was obtained in about 50% yield by the simple complexation of $CuCl_2$ and Hpz^{tBu} in basic MeOH.[7] The structure of **1** contains an unusual vertex-sharing $[\{Cu_3(Hpz^{tBu})_6(\mu_3\text{-}Cl)(\mu_3\text{-}OH)_3\}_2Cu]^{6+}$ double-cubane core, surrounded by a belt of six hydrogen-bonded Cl^- ions which are encapsulated within a hydrophobic sheath of *tert*-butyl groups. Vertex-sharing double-cubane complexes are still relatively unusual,[8–19] although interestingly one example is known containing a $[\{Cu_3(\mu_3\text{-}Cl)(\mu_3\text{-}OH)_3\}_2Cu]^{6+}$ core that is a structural isomer of the core in **1**.[18] Compound **1** represents an inversion of the usual scenario in polymetallic host–guest complexes, in that the chloride guests surround the periphery of the cluster core rather than being encapsulated within it. We now present a full account of the chemistry of **1** and of two related compounds containing other anion guests, and describe the products of similar reactions carried out using other copper(II) salts, intended to determine to what extent the structural topology of **1** depends on these supramolecular cation–anion interactions.

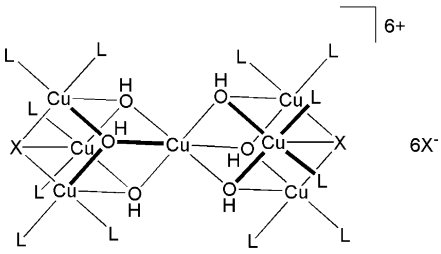

$X^- = Cl^-$, **1**
$X^- = Br^-$, **2**

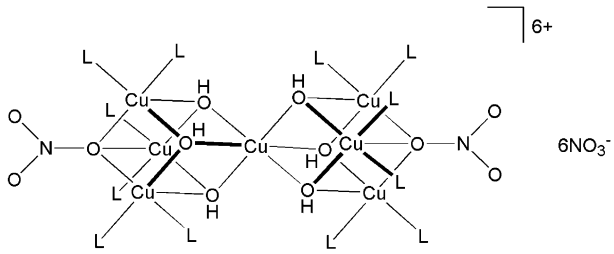

3

L = Hpz^{tBu}

Results and Discussion

Syntheses and crystal structures: Reaction of hydrated CuX_2 (X^-=Cl^-, Br^-, NO_3^-), NaOH and Hpz^{tBu} in a 1:1:2 molar ratio in MeOH at 293 K for three days yields a dark green solution. Evaporation to dryness and extraction of the residue with CH_2Cl_2 affords a dark green solution, which gives low-to-moderate yields of turquoise crystals upon layering with pentane. These products were identified as $[\{Cu_3(Hpz^{tBu})_6(\mu_3\text{-}X)(\mu_3\text{-}OH)_3\}_2Cu]X_6$ (X^-=Cl^-, **1**; X^-=Br^-, **2**; X^-=NO_3^-, **3**) by elemental analysis and crystallography (see below). The long reaction time seems necessary to maximize the yields of **1**–**3**, and to avoid contamination of the product by the corresponding monomers $[CuX_2(Hpz^{tBu})_4]$.[20] Pure **1** and **2** can be recrystallized cleanly from CH_2Cl_2–pentane mixtures; recrystallization of **3** results in partial decomposition of the sample. Importantly, **1**–**3** can *only* be prepared by slow crystallization. Rapid precipitation of these compounds from solution instead yields green powders that were not investigated in detail, but which appear to contain more than one complex product from their solubility properties. While single crystals of **1** and **2** both contain lattice solvent (CH_2Cl_2 and pentane, respectively), for both compounds this solvent is lost upon drying in vacuo to yield analytically pure solvent-free material. All magnetic and spectroscopic measurements on **1** and **2** were carried out using these dried compounds.

Although they are not isomorphous, the molecular structures of **1**[7] and **2** in their solvated crystals are very similar. The asymmetric unit of **2**·2C_5H_{12} contains half a complex molecule, with Cu(1) lying on a crystallographic inversion center, together with one molecule of pentane lying on a general position. The overall structure of the complex is of a $[\{Cu_3(Hpz^{tBu})_6(\mu_3\text{-}Br)(\mu_3\text{-}OH)_3\}_2Cu]^{6+}$ vertex-sharing double heterocubane (Table 1, Figure 1). The central Cu atom Cu(1) has a distorted octahedral $Cu(OH)_6$ coordination sphere with near-regular O-Cu(1)-O angles, while Cu(2)–Cu(4) exhibit *cis*-tetragonal geometries, with two basal OH^- and two Hpz^{tBu} ligands. The cubane moiety is completed by Br(62), which makes long axial contacts to each of Cu(2)–Cu(4). The six charge-balancing Br^- ions are disposed in an approximately C_3-symmetric ring around the double-cubane core of the molecule (Figure 2). Each of these Br^- ions forms a weak axial interaction to one Cu ion, and accepts hydrogen bonds from one OH^- and two Hpz^{tBu} N–H donors (Table 2). These weak interactions are disposed in a distorted pyramidal geometry about the Br centers (Figure 2), with *trans*-H···Br···H and H···Br···Cu angles ranging from 105.0–121.5°. The guest anions are additionally shielded from the environment by a hydrophobic shell of *tert*-butyl groups.

There are two main differences between the structures of **1** and **2** in their crystals. First, in **1** Cu(1) has a clearly Jahn–Teller elongated structure, with one of the three unique Cu(1)–O bonds being an average of 0.323(2) Å longer than the other two.[7] In contrast, the distribution of Cu(1)–O distances in **2** is more suggestive of a Jahn–Teller compressed octahedral geometry (Table 1).[21] However, a mean-square displacement amplitude (MSDA)[22] analysis of the bonds to Cu(1) in **2** strongly implies that the Cu(1)–O(6) and Cu(1)–O(7) bonds are disordered: the ΔMSDA values are Cu(1)–O(5) = 10, Cu(1)–O(6) = 188, and Cu(1)–O(7) = 194×10^{-4} Å^2. This is consistent with Cu(1) in **2** adopting a more common Jahn–Teller elongated geometry, as in **1**, with the axis of elongation being disordered between the O(6)-Cu(1)-O(6′) and O(7)-Cu(1)-O(7′) vectors (Figure 1).[21] For

Table 1. Selected bond lengths [Å] and angles [°] in the crystal structure of **2**·2 C_5H_{12}. The equivalent parameters are also listed for **1**·2 CH_2Cl_2,[7] for comparison.[a]

	1·2 CH_2Cl_2[b]	**2**·2 C_5H_{12}[c]		**1**·2 CH_2Cl_2[b]	**2**·2 C_5H_{12}[c]		**1**·2 CH_2Cl_2[b]	**2**·2 C_5H_{12}[c]
Cu(1)–O(5)	1.9781(13)	1.959(2)	O(5)-Cu(2)-O(6)	80.66(6)	81.91(10)	N(35)-Cu(3)-X(62)	92.62(5)	91.45(9)
Cu(1)–O(6)	1.9675(13)	2.121(3)	O(5)-Cu(2)-N(8)	94.23(6)	94.92(11)	N(35)-Cu(3)-X(64)	87.73(5)	87.27(9)
Cu(1)–O(7)	2.2957(13)	2.153(3)	O(5)-Cu(2)-N(17)	169.98(6)	173.15(11)	X(62)-Cu(3)-X(64)	179.544(18)	178.721(19)
Cu(2)–O(5)	1.9731(14)	1.991(2)	O(5)-Cu(2)-X(62)	92.03(4)	89.08(7)	O(5)-Cu(4)-O(7)	83.51(6)	82.55(10)
Cu(2)–O(6)	1.9862(13)	1.965(2)	O(5)-Cu(2)-X(63)	95.20(4)	91.18(7)	O(5)-Cu(4)-N(44)	176.82(6)	173.22(11)
Cu(2)–N(8)	1.9997(17)	1.989(3)	O(6)-Cu(2)-N(8)	166.64(6)	174.18(12)	O(5)-Cu(4)-N(53)	89.54(6)	89.25(11)
Cu(2)–N(17)	1.9889(18)	1.985(3)	O(6)-Cu(2)-N(17)	93.26(6)	93.48(12)	O(5)-Cu(4)-X(62)	84.43(4)	89.80(7)
Cu(2)–X(62)	2.5502(5)	2.7639(6)	O(6)-Cu(2)-X(62)	91.61(4)	91.95(7)	O(5)-Cu(4)-X(65)	89.13(4)	97.54(7)
Cu(2)–X(63)	3.7429(6)	3.5212(6)	O(6)-Cu(2)-X(63)	92.19(4)	97.32(7)	O(7)-Cu(4)-N(44)	94.54(6)	96.93(12)
Cu(3)–O(6)	1.9940(13)	1.971(2)	N(8)-Cu(2)-N(17)	89.95(7)	89.22(13)	O(7)-Cu(4)-N(53)	171.86(7)	169.95(12)
Cu(3)–O(7)	1.9549(14)	1.982(2)	N(8)-Cu(2)-X(62)	100.95(5)	92.89(9)	O(7)-Cu(4)-Br(62)	85.16(4)	89.46(7)
Cu(3)–N(26)	2.0096(18)	1.998(3)	N(8)-Cu(2)-X(63)	75.89(5)	77.80(9)	O(7)-Cu(4)-X(65)	98.12(4)	93.70(7)
Cu(3)–N(35)	1.9988(17)	1.997(3)	N(17)-Cu(2)-X(62)	96.13(5)	96.18(9)	N(44)-Cu(4)-N(53)	92.58(7)	90.54(13)
Cu(3)–X(62)	2.8641(5)	2.9717(6)	N(17)-Cu(2)-X(63)	76.97(5)	84.35(9)	N(44)-Cu(4)-X(62)	97.93(5)	96.96(9)
Cu(3)–X(64)	2.7938(5)	3.0807(6)	X(62)-Cu(2)-X(63)	172.30(2)	170.676(19)	N(44)-Cu(4)-X(65)	88.65(5)	75.72(9)
Cu(4)–O(5)	2.0076(14)	1.994(2)	O(6)-Cu(3)-O(7)	83.86(6)	82.97(11)	N(53)-Cu(4)-Br(62)	89.96(5)	96.35(9)
Cu(4)–O(7)	1.9493(13)	1.971(2)	O(6)-Cu(3)-N(26)	92.30(6)	94.13(12)	N(53)-Cu(4)-X(65)	85.97(5)	81.57(9)
Cu(4)–N(44)	2.0001(17)	1.987(3)	O(6)-Cu(3)-N(35)	173.98(6)	173.25(12)	X(62)-Cu(4)-X(65)	172.414(17)	172.319(19)
Cu(4)–N(53)	1.9999(17)	1.993(3)	O(6)-Cu(3)-X(62)	82.73(4)	85.85(7)	Cu(1)-O(5)-Cu(2)	96.61(6)	99.77(11)
Cu(4)–X(62)	2.7949(5)	2.7364(6)	O(6)-Cu(3)-X(64)	96.94(4)	95.42(7)	Cu(1)-O(5)-Cu(4)	102.33(6)	99.09(10)
Cu(4)–X(65)	2.9129(6)	3.5657(6)	O(7)-Cu(3)-N(26)	173.77(6)	176.44(11)	Cu(2)-O(5)-Cu(4)	108.97(6)	108.65(11)
O(5)-Cu(1)-O(6)	81.00(5)	78.80(10)	O(7)-Cu(3)-N(35)	91.81(6)	90.55(12)	Cu(1)-O(6)-Cu(2)	96.53(6)	95.27(10)
O(5)-Cu(1)-O(6′)	99.00(5)	101.20(10)	O(7)-Cu(3)-X(62)	83.16(4)	82.74(7)	Cu(1)-O(6)-Cu(3)	101.59(6)	98.70(11)
O(5)-Cu(1)-O(7)	75.74(5)	78.86(9)	O(7)-Cu(3)-X(64)	97.13(4)	97.20(7)	Cu(2)-O(6)-Cu(3)	111.11(6)	112.62(12)
O(5)-Cu(1)-O(7′)	104.26(5)	101.14(9)	N(26)-Cu(3)-N(35)	91.64(7)	92.26(13)	Cu(1)-O(7)-Cu(3)	92.12(5)	97.31(11)
O(6)-Cu(1)-O(7)	76.06(5)	75.59(9)	N(26)-Cu(3)-X(62)	91.50(5)	95.01(9)	Cu(1)-O(7)-Cu(4)	93.65(5)	93.55(10)
O(6)-Cu(1)-O(7′)	103.94(5)	104.41(9)	N(26)-Cu(3)-X(64)	88.19(5)	85.12(9)	Cu(3)-O(7)-Cu(4)	118.55(7)	115.57(12)

[a] Primed atoms are related to unprimed atoms in both structures by the relation $1-x$, $1-y$, $1-z$. [b] X = Cl. [c] X = Br.

Table 2. Metric parameters [Å, °] for the hydrogen bonds in the crystal structure of **2**·2 C_5H_{12}. The equivalent parameters are also listed for **1**·2 CH_2Cl_2,[7] for comparison.[a]

	H···X	Y···X (Y=N, O)	Y–H···X (Y=N, O)
for **1**·2 CH_2Cl_2 (X=Cl):			
O(5)–H(5)···Cl(64′)	2.16	3.1099(14)	159.0
O(6)–H(6)···Cl(65′)	2.09	3.0514(14)	161.8
O(7)–H(7)···Cl(63′)	2.18	3.1690(14)	170.9
N(9)–H(9)···Cl(64′)	2.65	3.3470(19)	137.0
N(18)–H(18)···Cl(63)	2.29	3.1349(19)	160.9
N(27)–H(27)···Cl(65′)	2.38	3.2352(18)	164.4
N(36)–H(36)···Cl(64)	2.45	3.1104(18)	132.0
N(45)–H(45)···Cl(63′)	2.34	3.1929(18)	164.8
N(54)–H(54)···Cl(65)	2.41	3.0975(18)	135.2
for **2**·2 C_5H_{12} (X=Br):			
O(5)–H(5)···Br(64′)	2.24	3.223(2)	166.7
O(6)–H(6)···Br(65′)	2.25	3.241(3)	169.8
O(7)–H(7)···Br(63′)	2.28	3.266(3)	168.9
N(9)–H(9)···Br(64′)	2.60	3.422(3)	155.5
N(18)–H(18)···Br(63)	2.48	3.295(3)	154.3
N(27)–H(27)···Br(65′)	2.52	3.374(3)	163.5
N(36)–H(36)···Br(64)	2.50	3.224(3)	140.3
N(45)–H(45)···Br(63′)	2.54	3.410(3)	170.4
N(54)–H(54)···Br(65)	2.42	3.237(3)	154.1

[a] Primed atoms are related to unprimed atoms in both structures by the relation $1-x$, $1-y$, $1-z$.

1, the three corresponding ΔMSDA values lie between 24–31×10^{-4} Å^2, confirming that this compound has a static geometry in the crystal. The known double-cubane $[\{Re_3(CO)_9(\mu_3\text{-}OH)_4\}_2Cu]$, which has a central $[Cu(OH)_6]^{4-}$ moiety, also exhibits a crystallographically ordered Jahn–Teller elongated Cu center.[13]

The second difference between **1** and **2** lies in the positions of the guest halide anions X(63)–X(65) (X=Cl or Br), which occupy two types of site depending on whether or not they form long-range axial contacts to one of Cu(2)–Cu(4). In **1**, the distances Cu(2)···Cl(63), Cu(3)···Cl(64), and Cu(4)···Cl(65) have a ′two short plus one long′ distribution (Table 1).[7] This is because Cl(63) is hydrogen-bonded to the OH^- ligand lying on the Jahn–Teller elongation axis of Cu(1), causing it to be displaced by 0.9 Å away from Cu(2) compared to the relative positions of Cl(64) and Cl(65) within the anion torus (Table 1). In contrast for **2**, the distances Cu(2)···Br(63), Cu(3)···Br(64), and Cu(4)···Br(65) now have a ′one short plus two long′ pattern. This reflects the disordered Jahn–Teller elongation axis at Cu(1) in **2**, since Br(63) and Br(65) hydrogen bond to the disordered OH^- ions O(6) and O(7) and are hence displaced away from their nearest neighbor Cu sites. Hence, it is unclear whether it is the packing of Br^- ions within the anion torus that causes the Jahn–Teller axis at Cu(1) to be disordered in **2**, or vice versa.

The structure of **3** also contains a $[\{Cu_3(Hpz^{tBu})_6(\mu_3\text{-}NO_3\text{-}\kappa^1)(\mu_3\text{-}OH)_3\}_2Cu]^{6+}$ double-cubane cation surrounded by six hydrogen-bonded NO_3^- ions, with a crystallographic inversion center at Cu(1) (Figure 1). In contrast to **1** and **2**, the cluster cation and anions in **3** are disordered about this inversion center, so that every atom in the crystal is disordered over two half-occupied positions referred to as ′A′ and ′B′ in Figure 1, except for Cu(1) and O(5)–O(7) (see the Experimental Section). A complete molecule of **3** is made up of one ′A′ half-molecule and one ′B′ half-molecule, linked by the shared-vertex Cu(1). Because of the large

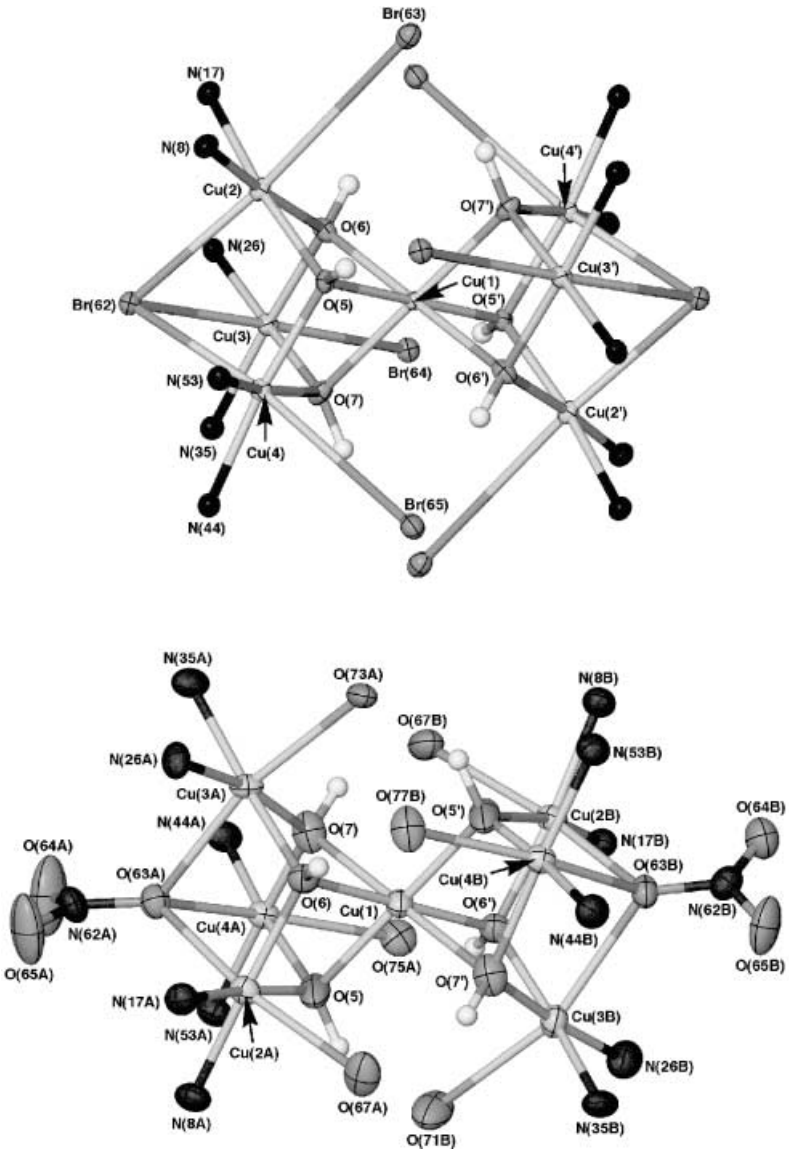

Figure 1. Views of the copper coordination environments of the $[\{Cu_3(Hpz^{tBu})_6(\mu_3\text{-}Br)(\mu_3\text{-}OH)_3\}_2Cu]Br_6$ and $[\{Cu_3(Hpz^{tBu})_6(\kappa^1,\mu_3\text{-}NO_3)(\mu_3\text{-}OH)_3\}_2Cu](NO_3)_6$ molecules in the crystal structures of **2**·2 C_5H_{12} (top) and **3** (bottom), showing the atom numbering scheme adopted. For clarity, only the coordinated N atoms of the Hpz^{tBu} ligands and, for **3**, the coordinated O atoms of the guest NO_3^- ions, are shown. Thermal ellipsoids are at the 35% probability level. The $[\{Cu_3(Hpz^{tBu})_6(\mu_3\text{-}Cl)(\mu_3\text{-}OH)_3\}_2Cu]Cl_6$ molecule in **1**·2 CH_2Cl_2 is visually very similar to that in **2**, and uses the same atom numbering scheme but with Br(62)–Br(65) replaced by Cl(62)–Cl(65).

number of restraints required to model this disorder, the bond lengths and angles within the structure cannot be relied on, and only the gross structural features of **3** will be considered.

One unusual feature of **3** is the $\mu_3\text{-}NO_3^-\text{-}\kappa O^1{:}\kappa O^1{:}\kappa O^1$ ligands, which form weak axial contacts to Cu(2)–Cu(4) (Figure 1). There is only one other example of a nitrato ligand with this coordination mode,[23] although a small number of compounds bearing a $\kappa^1,\mu_4\text{-}NO_3^-$ ion have also been described.[24–27] The disorder in **3** probably reflects non-complimentarity between the hydrogen-bond donors in the cluster cation, and the trigonal-planar NO_3^- guests. Each NO_3^- ion within the anion belt forms a weak axial interaction to one Cu center and accepts hydrogen bonds from one OH and two NH donors, as in **1** and **2**. However, the orientation of each anion within the belt is different (Figure 2). Five of the six guest nitrate ions accept one hydrogen bond at each O atom (Scheme 1, A); however, the sixth anion accepts two of its three hydrogen bonds at the same O atom, leaving one O atom protruding away from the cluster core (Scheme 1, B).

As we have already reported, the reaction of hydrated CuF_2 with Hpz^{tBu} under the same conditions used for **1**--**3** yields a very different product, of formula $[\{Cu_3(Hpz^{tBu})_4(\mu\text{-}pz^{tBu})_2(\mu\text{-}F)_2(\mu_3\text{-}F)\}_2]F_2$ (**4**).[28] This cyclic hexacopper complex contains two F^- ions that are bound supramolecularly to the complex in a similar manner as the guest anions in **1**–**3**. In the light of this novel result, several complexations of Hpz^{tBu} with other copper(II) salts in basic MeOH were also attempted. Only one of these gave noteworthy products. Following the procedure described for **1**–**3** using hydrated $Cu[BF_4]_2$ in the presence of excess NaNCS, yielded two crystalline compounds: *trans*-$[Cu(NCS)_2(Hpz^{tBu})_2]$ (**5**)[29] and $[Cu_2(NCS)_2(\mu\text{-}pz^{tBu})_2(\mu\text{-}Hpz^{tBu})(Hpz^{tBu})_2]$ (**6**). Complex **6** was the minor product of the reaction, and was always contaminated with **5** from which it had to be manually separated.

The structure of **6** is based around a typical puckered $[Cu_2(\mu\text{-}pz^{tBu})_2]^{2+}$ motif,[30] with the $[pz^{tBu}]^-$ bridging ligands disposed in a head-to-tail fashion. Remarkably, there is a $\mu\text{-}Hpz^{tBu}\text{-}\kappa N^2{:}\kappa N^2$ ligand lying within the resultant cleft, forming weak apical Cu–N contacts to both Cu ions (Table 3,

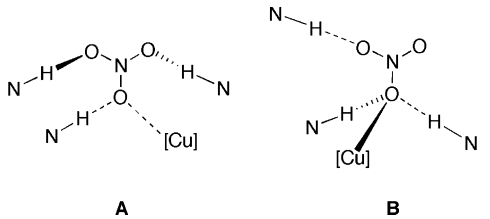

Scheme 1. Different patterns of supramolecular interactions to the guest NO_3^- ions in **3** (Figure 2).

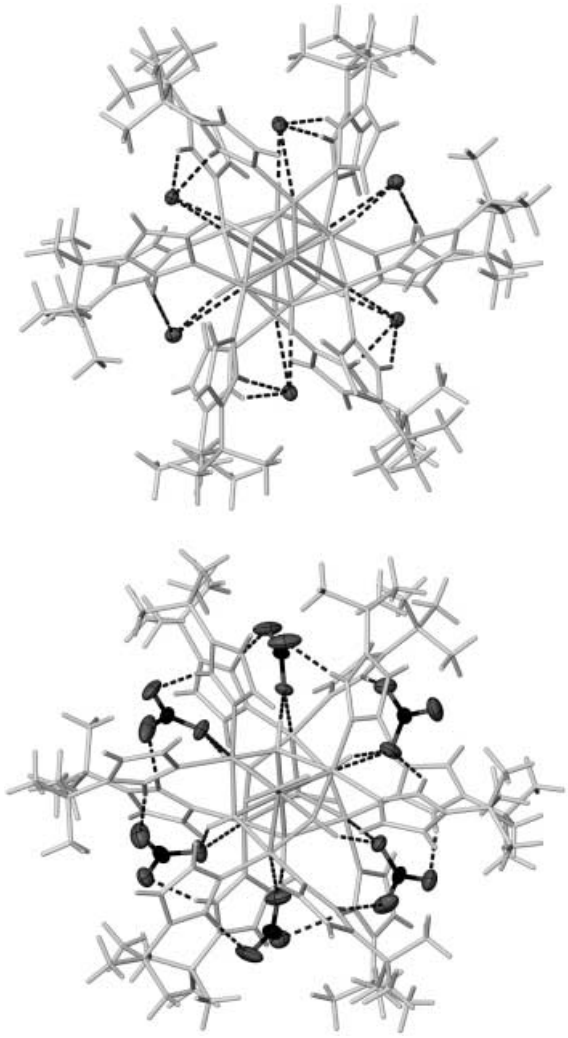

Figure 2. Views of the complete $[\{Cu_3(Hpz^{tBu})_6(\mu_3\text{-}Br)(\mu_3\text{-}OH)_3\}_2Cu]Br_6$ and $[\{Cu_3(Hpz^{tBu})_6(\kappa^1,\mu_3\text{-}NO_3)(\mu_3\text{-}OH)_3\}_2Cu][NO_3]_6$ molecules in the crystal structures of $\mathbf{2}\cdot 2C_5H_{12}$ (top) and **3** (bottom). The views are approximately parallel to the Br(62)···Cu(1)···Br(62′) vector for **2**, and the O(63)···Cu(1)···O(63′) vector for **3**. All hydrogen bonds and weak axial Cu···X (X=Br or O) interactions to the guest anions are highlighted. For clarity, only one orientation of the disordered *tert*-butyl groups in $\mathbf{2}\cdot 2C_5H_{12}$ is shown. Thermal ellipsoids are at the 35% probability level.

Figure 3). The dihedral angle between the bridging pyrazole ring N(45)–C(49) and the least-squares plane formed by Cu1, Cu(2), N(3), N(4), N(12), and N(13) is 88.90(9)°. This implies that the bridging pyrazole ligand interacts with both Cu(1) and Cu(2) through the N(45) lone pair, rather than coordinating to one metal ion through its π electrons.[31] Complexes of κ^1,μ azole ligands are very unusual.[32–34] In particular, this coordination mode has only been seen previously in one other transition metal complex of a neutral pyrazole donor, namely $[\{CuTp\}_2]$ ($[Tp]^-$ = hydrido-*tris*-pyrazolylborate),[32] and in a small number of main-group metal pyrazolide salts.[33] The three terminal Hpz^{tBu} ligands in **6** form three different types of intramolecular hydrogen bond (Figure 3): to the N atom of a thiocyanate ligand; to one N atom of a pyrazolide ring; and, a bifurcated hydrogen bond to both N atoms of the other pyrazolide ring. Unfortunately, the yield of **6** was too small for us to be able to characterize it further, beyond confirming its identity.

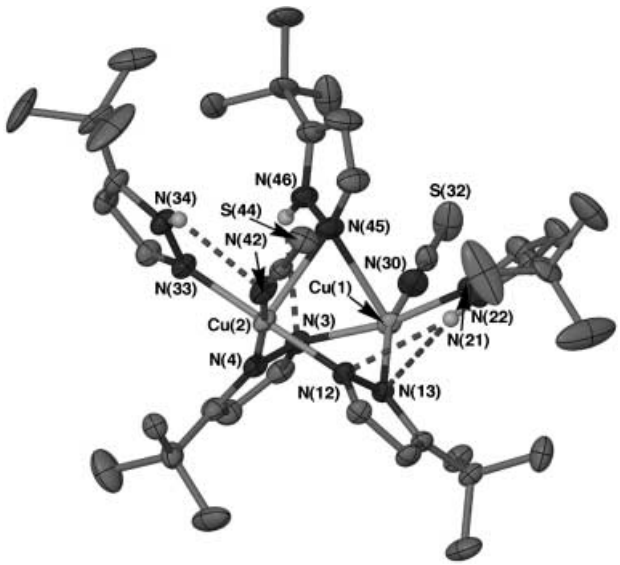

Figure 3. View of the $[Cu_2(NCS)_2(\mu\text{-}pz^{tBu})_2(\mu\text{-}Hpz^{tBu})(Hpz^{tBu})_2]$ molecule in the crystal structures of **6**. For clarity, all C-bound H atoms have been omitted while only the major orientation of the disordered *tert*-butyl groups is shown. Thermal ellipsoids are at the 35% probability level.

Table 3. Selected bond lengths [Å] and angles [°] in the crystal structure of **6**.

Cu(1)–N(3)	1.990(2)	Cu(2)–N(4)	1.988(2)
Cu(1)–N(13)	1.983(2)	Cu(2)–N(12)	1.957(2)
Cu(1)–N(21)	2.010(2)	Cu(2)–N(33)	2.010(2)
Cu(1)–N(30)	1.944(2)	Cu(2)–N(42)	1.975(2)
Cu(1)–N(45)	2.568(3)	Cu(2)–N(45)	2.483(3)
N(3)-Cu(1)-N(13)	91.09(9)	N(3)-Cu(1)-N(21)	165.67(10)
N(3)-Cu(1)-N(30)	92.84(11)	N(3)-Cu(1)-N(45)	81.40(9)
N(13)-Cu(1)-N(21)	88.79(9)	N(13)-Cu(1)-N(30)	158.82(10)
N(13)-Cu(1)-N(45)	100.03(9)	N(21)-Cu(1)-N(30)	92.42(11)
N(21)-Cu(1)-N(45)	84.51(9)	N(30)-Cu(1)-N(45)	101.13(10)
N(4)-Cu(2)-N(12)	89.18(9)	N(4)-Cu(2)-N(33)	90.89(9)
N(4)-Cu(2)-N(42)	168.92(10)	N(4)-Cu(2)-N(45)	94.12(9)
N(12)-Cu(2)-N(33)	179.32(9)	N(12)-Cu(2)-N(42)	90.43(9)
N(12)-Cu(2)-N(45)	92.90(8)	N(33)-Cu(2)-N(42)	89.63(9)
N(33)-Cu(2)-N(45)	86.41(9)	N(42)-Cu(2)-N(45)	96.96(10)

Solid-state magnetic properties: The variable-temperature magnetic behavior of **1**–**3** is very similar. At 300 K, $\chi_M T$ for all three compounds is 2.43(2) $cm^3 mol^{-1} K$, which is smaller than that expected for seven non-interacting $S=1/2$ copper(II) ions with a sensible g value ($\chi_M T = 2.86\ cm^3 mol^{-1} K$ for $g=2.1$).[35] As the temperature is lowered $\chi_M T$ decreases, reaching a plateau of 0.45(1) $cm^3 mol^{-1} K$ at 15 K (Figure 4), which is close to the value expected for a $S=1/2$ copper(II) species ($\chi_M T = 0.41\ cm^3 mol^{-1} K$ for $g=2.1$).[35] Hence, it is clear that antiferromagnetic superexchange is dominant in these compounds, leading to a $S=1/2$ ground state that is essentially fully populated below 15 K. After several unsatisfactory attempts using higher-symmetry models, these data were successfully fit using the following Hamiltonian [Eq. (1), Scheme 2].[7]

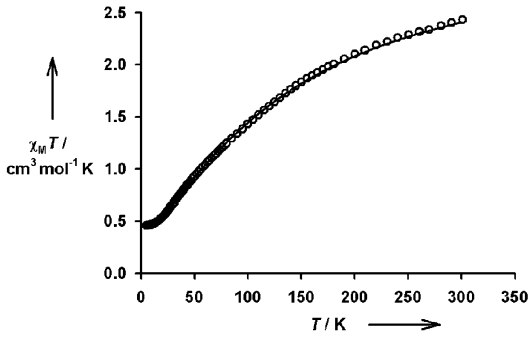

Figure 4. Plot of $\chi_M T$ versus T for a powder sample of **3**. The line shows the best fit to the model derived from Equation (1). See text for details. The $\chi_M T$ versus T curves for **1** and **2** are visually very similar to this graph.

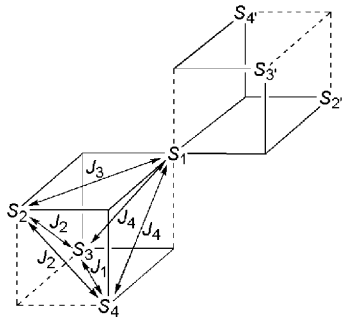

Scheme 2. Exchange coupling scheme employed to analyze the magnetic data of **1**–**3**. Each spin equates to the correspondingly numbered Cu ion in Figure 1 [that is, $S_1 \equiv$ Cu(1) etc.]. The solid and dotted lines linking the S centers correspond to equatorial and axial Cu–ligand bonds, respectively.

$$H = -2J_1(S_3S_4 + S_{3'}S_{4'}) - 2J_2(S_2S_3 + S_2S_4 + S_{2'}S_{3'} + S_{2'}S_{4'}) - 2J_3(S_1S_2 + S_1S_{2'}) - 2J_4(S_1S_3 + S_1S_4 + S_1S_{3'} + S_1S_{4'}) \quad (1)$$

All three datasets gave values of J_2 and J_4 that were approximately equal and, particularly for **1** and **2**, strongly correlated with each other. Hence, these two J values were constrained to be equal for the final calculations, which had no detectable effect on the quality of the fits. The final parameters from these analyses are listed in Table 4. As expected, **1**–**3** all have the same $S = {}^1/_2$ magnetic ground state, that is separated from a $S = {}^1/_2$ first excited state by 33–53 cm^{-1}. The identity of this first excited state is different for **3** compared to **1** and **2**, however, owing to the differences in the J values shown by the compounds.

Table 4. Results of fitting the magnetic data of **1**–**3**. The J-values correspond to those in Scheme 2, and are quoted in cm^{-1}. Further details of the procedures used are given in the text. Estimated errors on g are $\pm$ 0.01, on J_1 and J_3 are ± 1 cm^{-1}, and on J_2 and J_4 are ± 5 cm^{-1}.

	g	J_1	$J_2 = J_4$	J_3
1	2.14	−72	−16	−21
2	2.22	−73	−26	−27
3	2.22	−65	−34	−17

The constant J_3 describes superexchange mediated by two OH^- ligands that both lie in the xy magnetic planes of Cu(1) and Cu(2). The value for this coupling in **1** agrees well with Haase's correlation for basal–basal superexchange in $[Cu_4(\mu_3\text{-}OR)_4]^{4+}$ (R = alkyl) cubanes, which predicts $J_3 \sim -30$ cm^{-1} for the observed average Cu(1)-O-Cu(2) angle in **1** of 96.57(8)°.[36] The corresponding angles in **2** and **3** cannot be derived accurately, because of the librational disorder at Cu(1) in **2** and the crystallographic disorder in **3**. The other superexchange constants J_1, J_2, and J_4 are mediated by one equatorial-equatorial $[Cu_2(\mu\text{-}OH)]^{3+}$ bridge, and a second equatorial–axial hydroxide bridging ligand that should contribute negligibly to superexchange between these Cu ions.[36] Despite the structural disorder in **2** and **3**, it is clear that the equatorial-equatorial Cu-O-Cu angles across these bridges in **1**–**3** follow the trend: Cu(3)-O(7)-Cu(4) $\gg$ Cu(2)-O(6)-Cu(3) ~ Cu(2)-O(5)-Cu(4) > Cu(1)-O(6)-Cu(3) ~ Cu(1)-O(5)-Cu(4). Hence, it can be predicted that J_1 should be more antiferromagnetic than J_2 or J_4,[37] in agreement with our results.

For **1** and **2**, the observed J values follow the order $|J_1| > |J_3| = |J_2, J_4|$; in contrast, for **3** the ordering is $|J_1| > |J_2, J_4| > |J_3|$. Both these orderings result in S_1, S_2, and $S_{2'}$ being spin-frustrated with respect to S_3, S_4, $S_{3'}$, and $S_{4'}$ (Scheme 2) when J_1 is antiferromagnetic. This is demonstrated by the equation for the energy of the magnetic ground state of the compounds, which depends on J_1 and J_3 only [Eq. (2)].

$$E_0 = 2J_3 + 3J_1 \quad (2)$$

That is, the ground state is equivalent to two antiferromagnetically coupled dimers of spins (S_3, S_4 and $S_{3'}$, $S_{4'}$) and an antiferromagnetically coupled trimer (S_1, S_2, $S_{2'}$) that are magnetically independent of each other within the molecule. This is discussed further below. For the same reasons, it is also reasonable that J_2 and J_4, which connect these discrete spin systems within the molecules, should be poorly defined by the susceptibility data.

Support for the assignment of the ground states of **1**–**3** comes from EPR spectroscopy of **1** and **2**. At room temperature, these compounds gave rise to very broad, unresolved spectra. The spectra sharpen upon cooling until, at temperatures below about 20–30 K, a rhombic $S = {}^1/_2$ spectrum is observed as the ground state is populated exclusively. On further cooling to 5 K an eight-line hyperfine pattern is observed in the "parallel" region (Figure 5). The low-temperature spectra can be interpreted in terms of an exchange-coupled linear trimer, as predicted by the model used to interpret the magnetic susceptibility data (see above). We treat the ground state as arising from the antiferromagnetic exchange interactions within the Cu(2)···Cu(1)···Cu(2′) fragment (S_2, S_1, $S_{2'}$). In these circumstances the ground state is expected to be $|1, {}^1/_2>$ in the $|S_2S_{2'}, S_T>$ notation, where S_T is the total spin. The hyperfine coupling (A_k^S) to each of the individual Cu ions k in the ground state is given by vector coupling of the single-ion hyperfines by using Equation (3),[38] where the spin-projection coefficients c_i are calculated from S_2, $S_{2'}$, S_1, $S_2S_{2'}$ and S_T.

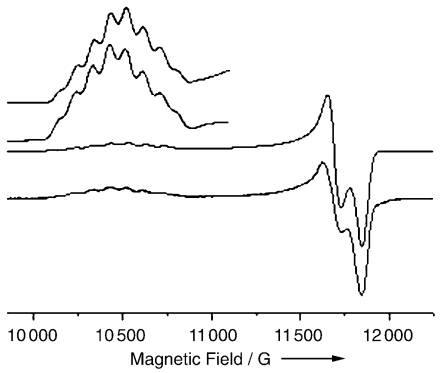

Figure 5. Experimental (lower) and simulated (upper) *Q*-band EPR spectrum of polycrystalline **1** at 4.2 K. See text for simulation parameters. Inset: experimental (lower) and simulated (upper) expansion of $g_{\|}$ region.

$$A_k^S = c_1 A_k^{Cu(2)} + c_2 A_k^{Cu(2')} + c_3 A_k^{Cu(1)} \quad (3)$$

When calculating the hyperfine to any given nucleus it is assumed that only one term in Equation (3) is retained (i.e. the coupling of the nucleus of one Cu ion to the electrons of another is small).[38] For example, the hyperfine to Cu(2), $A_{Cu(2)}^S$ is given by $c_1 A_{Cu(2)}^{Cu(2)}$, with $A_{Cu(2')}^{Cu(2)} = A_{Cu(1)}^{Cu(2)} = 0$. For the $|1, {}^1/_2>$ ground state of a trimer of $S = {}^1/_2$, the coefficients are $c_1 = c_2 = {}^2/_3$, $c_3 = -{}^1/_3$.[38] That is, the hyperfine to the outer two nuclear spins should be equal, and $^2/_3$ the value of their single-ion values, while the coupling to the central nuclear spin should be $-{}^1/_3$ that of its single-ion value.

In **1**–**3** the Jahn–Teller axes of Cu(1), Cu(2), and Cu(2′), and therefore their A_{zz} axes (where A_{zz} is the largest hyperfine interaction), are approximately co-parallel with each other and with the ground state A_{zz}. In the assumption that the single-ion hyperfines of these three centers are equal [those of Cu(2) and Cu(2′) are required to be by symmetry], we would expect the hyperfine couplings in the ground state to involve two identical interactions with two $I = {}^3/_2$ nuclei and a coupling of half this magnitude to a third $I = {}^3/_2$ nucleus. The low temperature spectra of **1** and **2** can indeed be simulated with this kind of pattern (Figure 5). The derived parameters are: for **1** $g_{zz} = 2.324(2)$, $g_{xx} = 2.084(2)$, $g_{yy} = 2.056(2)$, $A_{zz}^{Cu(2)/Cu(2')} = 90(3)$ G, $A_{zz}^{Cu(1)} = 36(3)$ G; and for **2** $g_{zz} = 2.315(2)$, $g_{xx} = 2.078(2)$, $g_{yy} = 2.050(2)$, $A_{zz}^{Cu(2)/Cu(2')} = 100(3)$ G, $A_{zz}^{Cu(1)} = 40(3)$ G. A_{xx} and A_{yy} were held at arbitrarily small values of 5 G, while isotropic Gaussian line-widths of 50 G were used. The simulations are insensitive to the relative signs of the hyperfines, but are very sensitive to the ratio of $A_{zz}^{Cu(2)/Cu(2')}$:$A_{zz}^{Cu(1)}$. When this ratio is less than 2:1 an irregular ten-line multiplet is observed (at line-widths similar to those observed experimentally), while above ca. 4:1 a regular seven-line multiplet is observed. The experimental ratios of the hyperfine interactions are 2.5:1, in good agreement with that predicted by the spin projection model [assuming similar single-ion A_{zz} values for Cu(2)/Cu(2′) and Cu(1)], and provide convincing support for the exchange coupling scheme used to model the magnetic data.

Solution studies: The turquoise solids **1**–**4** form green or khaki-colored solutions that are markedly solvatochromic. For example, the d–d maximum shown by **2** spans the range 683 (530) $\leq \lambda_{max}$ [nm] (ε_{max} [M^{-1} cm^{-1}]) $\leq$ 785 (920) in C_7H_8, CH_2Cl_2, MeCN, and $(CH_3)_2CO$; a similarly wide range in λ_{max} is exhibited by the other compounds in these solvents. These data show that the structures of **1**–**4** in solution are solvent-dependent, and hence not the same as in the solid state. For this reason, more detailed solution characterization of **1**–**4** was not undertaken.

The above conclusions were also borne out by mass spectrometric data from **1**, **2**, and **4**, which only exhibited low-molecular-weight fragments. Three different ionization techniques were studied: fast atom bombardment (FAB, 3-nitrobenzylalcohol [NOBA] matrix), electrospray (ES, CH_2Cl_2/MeOH matrix), and matrix-assisted laser desorption/ionization (MALDI, *trans*-1,1-dicyano-3-methyl-4-[4-*tert*butylphenyl]buta-1,3-diene [DCTB] matrix). The FAB spectra showed significant copper-containing molecular ions corresponding to $[^{63}Cu(Hpz^{tBu})]^+$ (*m*/*z* 187), $[^{63}Cu(Hpz^{tBu})_2]^+$ (311) and $[^{63}Cu_2(Hpz^{tBu})_2X]^+$ (X=^{35}Cl, 409; X=^{79}Br, 453; X=^{19}F, 393) only. Similarly, the ES spectra exhibited only the aforementioned peak at *m*/*z* 311, together with a new peak from $[^{63}Cu(Hpz^{tBu})_3X+H]^+$ (X=^{35}Cl, 471; X=^{79}Br, 515; X=^{19}F, 455). The MALDI analyses showed strong ions corresponding to $[^{63}Cu(DCTB)]^+$ (*m*/*z* 313) and $[^{63}Cu(DCTB)_2]^+$ (563), showing that the samples had reacted with the matrix. These were not therefore analyzed further. The absence of any high-nuclearity ions in these spectra, and the reactivity of the samples towards the MALDI matrix, both confirm the conclusion that these compounds do not retain their solid-state structures upon dissolution.

Conclusions

We have characterized the molecular structures and magnetochemistry of a series of heptacopper double-cubane compounds, containing supramolecularly bound Cl^-, Br^-, or NO_3^- ions. The guest ions are bound to the cluster molecules through a combination of hydrogen-bonding, hydrophobic interactions, and axial interactions to the Cu centers. While few data are available, measured enthalpies of axial copper(II)–ligand bonds to moderately or weakly basic ligands range from about 5–60 kJ mol^{-1}.[39] In addition, the Cu···X (X=Cl or Br) distances to the guest ions are 0.25(9)–1.20(9) Å (Cl) and 0.43(12)–0.92(12) Å (Br) longer than the median axial Cu···X distances in the Cambridge Crystallographic Database in 1989 [Cu···Cl=2.54(9), Cu···Br=2.65(12)].[40] So, these axial interactions in **1** and **2**, at least, should be weaker than average. For these reasons, we believe that the Cu···X interactions to the guest anions in **1**–**3** will be of the same order as the three N–H···X hydrogen bonds per X^- ion (ca. 15 kJ mol^{-1} per hydrogen bond in one metal complex with a similar geometry of N–H···Cl hydrogen bonding[41]). Hence, we regard **1**–**3** as genuine supramolecular anion complexes. The identity of the guest anion controls the products of the reactions, in that the double-cubane structure is obtained when Cl^-, Br^-, or NO_3^- is the

counterion present, but not for F^-, NCS^-, or any of the other anions we investigated (N_3^-, $MeCO_2^-$, BF_4^-, ClO_4^- etc.). However, since **1**–**3** apparently decompose to mixtures of low nuclearity copper(II) species in solution, it is uncertain to what degree their structures are templated by these exogenous anions.

It is interesting that **1**–**3** represent a third known structural type for heptacopper vertex-sharing double cubanes with a $[\{Cu_3(\mu_3\text{-}OH)_3(\mu_3\text{-}Y)\}_2Cu]^{6+}$ (Y^-=OH^-, Cl^-, Br^-, or NO_3^-) core (Scheme 3).[12,18] These structures differ in the

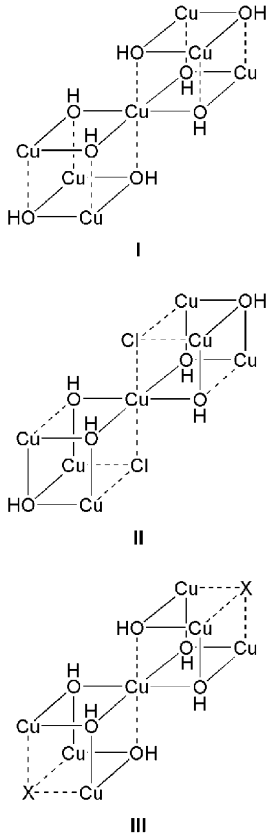

Scheme 3. Topologies of equatorial (solid lines) and axial (dotted lines) copper–ligand bonding in the vertex-sharing double cubanes: $[\{Cu_3(bpym)_3(OH_2)(\mu_3\text{-}OH)_4\}_2Cu][NO_3]_6$ (bpym = 2,2′-bipyrimidine, **I**);[12] $[\{Cu_3(pn)_3(OH_2)(\mu_3\text{-}OH)_3(\mu_3\text{-}Cl)\}_2Cu][C(CN)_3]_4Cl_2$ (pn = 1,3-diaminopropane, **II**);[18] and **1**–**3** (X^- = Cl^-, Br^-, or NO_3^-, **III**).

dispositions of apical or axial copper ligand bonds within the individual cubane moieties. The two distinct cubanes in structure **I** in Scheme 3 can be thought of as dimers of $[Cu_2(\mu\text{-}OH)_2]^{2+}$ dimers linked by weak axial Cu···O interactions. This is a common structural type in $[Cu_4(\mu_3\text{-}OR)_4]^{4+}$ (R=H, alkyl) cubane chemistry.[36,42] The individual cubane moieties in structures **II** and **III** have more complex structures, that have no precedent in Jahn–Teller distorted cubane compounds. Despite these differences in molecular structure, however, spin frustration effects mean that all the known $[\{Cu_3(\mu_3\text{-}OH)_3(\mu_3\text{-}Y)\}_2Cu]^{6+}$ compounds have the same *magnetic* ground-state structure,[12,18] of a pair of dimers [Cu(3), Cu(4) and their symmetry equivalents for **1**–**3**, Figure 1] and a trimer [Cu(1), Cu(2), and Cu(2′)] that are magnetically independent of one another. This means that structures **II** and **III** in Scheme 3 give rise to a magnetic ground state equivalent to structure **I**. The EPR spectra of **1** and **2** at 5 K confirm this interpretation, by showing hyperfine coupling to three Cu centers only. The antiferromagnetically coupled pairs Cu(3), Cu(4) and Cu(3′), Cu(4′) will be EPR-silent, and so will not contribute to the ground-state EPR spectrum. Unusually for polynuclear copper(II) complexes, the hyperfine structure in the $S=\frac{1}{2}$ ground state is resolved in low-temperature EPR spectra. The hyperfine multiplets consist of eight lines, which is a consequence of the relative values of the hyperfine couplings to the three individual copper(II) ions that contribute to the ground state. These values can be rationalized by a spin projection of the single-ion hyperfines. To the best of our knowledge this is the first time that this has been possible for a copper(II) cluster with nuclearity greater than two, although related phenomena have been noted in the EPR spectra of biological polynuclear manganese centers.[43] A similar EPR study has also recently been reported, of the localization of a $S=\frac{1}{2}$ ground state onto a single metal ion in a spin-frustrated tricopper(II) compound.[44]

Experimental Section

Instrumentation: Elemental microanalyses were performed by the University of Leeds School of Chemistry microanalytical service. Fast atom bombardment mass spectra were obtained on a VG Autospec instrument, using a 3-nitrobenzylalcohol matrix. Electrospray mass spectra were obtained on a Waters ZQ4000 spectrometer, in a CH_2Cl_2/MeOH solvent mixture. MALDI mass spectra were run using an Applied Biosystems Voyager DE-STR TOF spectrometer, with a *trans*-1,1-dicyano-3-methyl-4-[4-*tert*-butylphenyl]buta-1,3-diene matrix. UV/Vis measurements were performed by using a Perkin Elmer Lambda900 spectrophotometer, in 1 cm quartz solution cells. *Q*-band EPR spectra were obtained using a Bruker ESP300E spectrometer fitted with an ER5106QT resonator and ER4118 VT cryostat. Spectral simulations were performed using in-house software which has been described elsewhere.[45] EPR measurements were performed on lightly ground crystals of **1**–**3**, because vigorous grinding of the crystals led to their decomposition, as evidenced by a darkening of the solid and the appearance of a simple near-axial monomeric copper(II), $S=\frac{1}{2}$ spectrum at all temperatures with $g_\parallel = 2.29$, $g_\perp = 2.06$ and $A_\parallel(^{63,65}Cu) = 160$–$170$ G; and because the compounds could not be prepared as homogeneous powders (see above). Despite this, the spectra obtained from **1** and **2** are the true powder spectra, as evidenced by their lack of change on rotating the sample in the magnetic field. For **3**, the monomeric copper(II) signal was observed even following very light grinding of the sample; therefore, a detailed EPR study of this complex was not possible.

Susceptibility measurements were performed on a Quantum Design SQUID magnetometer, in an applied field of 2000 G. A diamagnetic correction for the sample was estimated from Pascal's constants;[35] a diamagnetic correction for the sample holder was also applied. The Hamiltonian matrix [Eq. (1)] was calculated in the coupled-spins representation, in which it can be made block-diagonal. The blocks were independently diagonalized by using MAPLE[46] (with the RACAH package for angular momentum algebra[47]), leading to analytical equations for the energies of their eigenstates and their derivatives. These expressions were used in a non-linear fit of the van Vleck equation to $\chi_M T$, using an iterative procedure based on the Marquadt method.[48] No paramagnetic impurity or TIP term was included in the final analysis. The errors on the fitted parameters were estimated from their reproducibility in other local minima of the fitting process.

Materials and methods: All reactions were carried out in air, using non-pre-dried AR-grade solvents. 3{5}-*tert*-Butylpyrazole (Hpz^{tBu}),[49] $[\{Cu_3(Hpz^{tBu})_6(\mu_3\text{-}Cl)(\mu_3\text{-}OH)_3\}_2Cu]Cl_6$ (**1**)[7] and $[\{Cu_3(Hpz^{tBu})_4(\mu\text{-}pz^{tBu})_2(\mu\text{-}F)_2(\mu_3\text{-}F)\}_2]F_2$ (**4**)[28] were prepared by the literature procedures, while all metal salts were used as supplied.

Synthesis of $[\{Cu_3(Hpz^{tBu})_6(\mu_3\text{-}Br)(\mu_3\text{-}OH)_3\}_2Cu]Br_6$ (2): A solution of NaOH (0.040 g, 1.0×10^{-3} mol) and 3{5}-*tert*-butylpyrazole (0.24 g, 2.0×10^{-3} mol) in MeOH (20 mL) was added to a mixture of $CuBr_2$ (0.22 g, 1.0×10^{-3} mol) in MeOH (30 mL). The resultant dark green solution was stirred at 293 K for three days, then evaporated to dryness. Extraction of soluble material from the residue with CH_2Cl_2, and layering of the resultant green solution with pentane, yields turquoise microcrystals of **2**. Recrystallization from CH_2Cl_2/pentane yielded very small, but strongly diffracting, rectangular prisms of formula $\mathbf{2}\cdot2C_5H_{12}$ which rapidly desolvated upon exposure to air. Yield 0.18 g, 47% based on Cu. Elemental analysis calcd (%) for $C_{84}H_{150}Br_8Cu_7N_{24}O_6$: C 37.7, H 5.7, N 12.6; found: C 37.8, H 5.7, N 12.4.

Synthesis of $[\{Cu_3(Hpz^{tBu})_6(\kappa^1,\mu_3\text{-}NO_3)(\mu_3\text{-}OH)_3\}_2Cu][NO_3]_6$ (3): Method as for **2**, using $Cu(NO_3)_2\cdot5H_2O$ (0.28 g, 1.0×10^{-3} mol). The product formed turquoise solvent-free crystals from CH_2Cl_2/pentane. Yield 0.080 g, 21% based on Cu. Elemental analysis calcd (%) for $C_{84}H_{150}Cu_7N_{32}O_{30}$: C 39.8, H 6.0, N 17.7; found: C 39.8, H 6.0, N 17.9.

Syntheses of $[Cu(NCS)_2(Hpz^{tBu})_2]$ (5) and $[Cu_2(NCS)_2(\mu\text{-}pz^{tBu})_2(\mu\text{-}Hpz^{tBu})(Hpz^{tBu})_2]$ (6): A solution of NaOH (0.040 g, 1.0×10^{-3} mol) and 3{5}-*tert*-butylpyrazole (0.24 g, 2.0×10^{-3} mol) in MeOH (20 mL) was added to a suspension of hydrated $Cu(BF_4)_2$ (0.32 g, 1.0×10^{-3} mol) in MeOH (20 cm^3). A solution of NaNCS (0.19 g, 2.4×10^{-3} mol) in MeOH (20 mL) was then added, and the mixture stirred at 293 K for 16 h. The solution was evaporated to dryness, the residue extracted with CH_2Cl_2 and the filtered blue solution layered with pentane to give large navy blue crystals of **5**. Yield 0.18 g, 54%. Elemental analysis calcd (%) for $C_{16}H_{24}CuN_6S_2$: C 44.9, H 5.7, N 19.6; found: C 44.9, H 5.8, N 19.9. The filtrate was left to evaporate slowly, yielding more crystals of **5** contaminated with a small number of green crystals of **6**, which were manually separated from this mixture. Yield 0.034 g, 8% based on Cu. Elemental analysis calcd (%) for $C_{37}H_{58}Cu_2N_{12}S_2$: C 51.5, H 6.8, N 19.5; found: C 51.6, H 6.8, N 19.5.

X-ray data collection and structural determinations: All diffraction measurements were performed on a Nonius KappaCCD area detector diffractometer equipped with an Oxford Cryosystems low-temperature device, using $Mo_{K\alpha}$ radiation ($\lambda=0.71073$ Å). Crystallographic data for each structure are summarized in Table 5. The unit cell of each structure was refined using all data. The structure of $\mathbf{2}\cdot2C_5H_{12}$ was solved by a Patterson synthesis,[50] while all the other structures were solved by direct methods.[50,51] Each of the initial models was developed by least-squares refinement on F^2;[52] the refinement of each structure is described in more detail below. MSDA calculations were performed using the program THMA11,[22] embedded into the PLATON suite of crystallographic software.[53]

CCDC-216810 ($\mathbf{2}\cdot2C_5H_{12}$), CCDC-216811 (**3**), CCDC-216812 (**5**), and CCDC-216809 (**6**) contain the supplementary crystallographic data for this paper. These data can be obtained free of charge via www.ccdc.cam.ac.uk/conts/retrieving.html (or from the Cambridge Crystallographic Centre, 12 Union Road, Cambridge CB2 1EZ, UK; Fax: (+44) 1223-336033; or deposit@ccdc.cam.ac.uk).

The asymmetric unit of $\mathbf{2}\cdot2C_5H_{12}$ contains half a molecule of the complex with Cu(1) lying on a crystallographic inversion center, and one molecule of pentane lying on a general position. The *tert*-butyl substituent C(40)–C(42) is disordered over two orientations labeled ′A′ and ′B′ with a 0.70:0.30 occupancy ratio, while the pentane molecule is disordered over two equally occupied orientations. All disordered C–C distances in the model were restrained to 1.53(2) Å, and nonbonded 1,3-C···C distances within a given disorder orientation to 2.50(2) Å. All non-H atoms with occupancy >0.5 were refined anisotropically, while all H atoms were placed in calculated positions and refined by using a riding model, except that the torsions of the methyl groups in the minor orientation of the disordered *tert*-butyl moiety were not allowed to refine.

The asymmetric unit of **3** contains half a molecule of the complex with Cu(1) lying on a crystallographic inversion center. High thermal parameters on the non-H atoms and a large number of residual Fourier peaks during initial refinement demonstrated that the whole half-molecule is disordered over two equally occupied orientations, referred to as ′A′ and ′B′. Every atom in the refinement apart from Cu(1) (which is crystallographically ordered on its special position) and O(5)–O(7) was thus refined in two half-occupied sites, using the following refined restraints: N–N = 1.34(2), N=C = 1.34(2), N–C = 1.35(2), C=C = 1.37(2), pyrazole C-C = 1.39(2), *tert*-butyl C–C = 1.52(2), *tert*-butyl 1,3-C···C = 2.48(2), N–O = 1.24(2), 1,3-O···O = 2.15(2) Å. No restraints were applied to the Cu–N or Cu–O bonds. It is likely that O(5)–O(7) should also be disordered; consistent with this, there are three residual electron density peaks of 1.3–1.4 e Å^{-3} in the vicinities of these atoms. However, they are not in an appropriate place to be considered as alternative disorder sites it for O(5)–O(7), and it proved impossible to refine distinct partial environments for these O atoms. Hence, O(5)–O(7) were left as wholly occupied in the final model. Similarly, high thermal parameters on some of the partial *tert*-butyl groups suggest that these are also disordered, although this could not be modeled. All non-H atoms with occupancy were refined anisotropically except for the aforementioned disordered partial *tert*-butyl environments C(13A)–C(16A), C(22B)–C(25B), C(40B)–C(43B), and

Table 5. Experimental details for the single-crystal structure determinations in this study.

	$\mathbf{2}\cdot2C_5H_{12}$	**3**	**5**	**6**
formula	$C_{94}H_{174}Br_8Cu_7N_{24}O_6$	$C_{84}H_{150}Cu_7N_{32}O_{30}$	$C_{16}H_{24}CuN_6S_2$	$C_{37}H_{58}Cu_2N_{12}S_2$
M_r	2820.63	2533.14	428.07	862.15
crystal class, space group	monoclinic, $P2_1/c$	triclinic, $P\bar{1}$	monoclinic, $P2_1$	orthorhombic, *Pbca*
a [Å]	12.3229(1)	14.2664(2)	5.8675(1)	12.5118(1)
b [Å]	15.9091(2)	16.5432(2)	10.1283(2)	17.3932(1)
c [Å]	32.0710(4)	16.5838(2)	17.3175(4)	41.7863(3)
α [°]	–	119.4961(6)	–	–
β [°]	97.4540(5)	97.7594(6)	91.7061(8)	–
γ [°]	–	95.8939(5)	–	–
V [Å^3]	6234.27(12)	3309.92(7)	1028.68(4)	9093.55(11)
Z	2	1	2	8
T [K]	100(2)	150(2)	150(2)	150(2)
μ [mm^{-1}]	3.789	1.176	2.278	1.066
ρ_{calcd}, [Mg m^{-3}]	1.503	1.271	1.510	1.259
measured reflections	47031	63845	9438	68921
independent reflections	14010	14714	4216	10351
R_{int}	0.056	0.065	0.046	0.098
R_1,[a] wR_2[b]	0.042, 0.095	0.068, 0.223	0.029, 0.078	0.047, 0.147
peak/hole [e Å^{-3}]	0.69/–0.51	1.45/–0.42	0.26/–0.25	0.65/–0.54
Flack parameter	–	–	0.477(8)[c]	–

[a] $R_1=\Sigma[|F_o|-|F_c|]/\Sigma|F_o|$. [b] $wR_2=[\Sigma w(F_o^2-F_c^2)^2/\Sigma wF_o^4]^{1/2}$. [c] This crystal was refined as a racemic twin.

C(49B)–C(52B). All H atoms were placed in calculated positions and refined by using a riding model.

Individual pyrazole ligands and nitrate ions in **3** were assigned to orientation ′A′ or ′B′ according to their distances from the relevant Cu atoms, and/or so as to avoid unfavorable inter-ligand steric contacts within each half-molecule. Whole molecules made up of two ′A′ or two ′B′ half-molecules all show a number of unfavorable C···C contacts between *tert*-butyl groups on opposite sides of the molecule. No such contacts occur in a molecule comprising one ′A′ and one ′B′ half-molecule. We therefore interpret this disorder as showing that each molecule in the lattice comprises one ′A′ and one ′B′ half-molecule linked through Cu(1), and that the molecule is disordered about the crystallographic inversion center. Consistent with this, an attempt to refine the structure in *P*1 led to a badly correlated model, in which the disorder was still present. Therefore, refinement in $P\bar{1}$ is correct.

The asymmetric unit of **5** contains one complex molecule lying on a general position. No disorder was detected during the refinement of this structure, and no restrains were applied. All non-H atoms were refined anisotropically, while all H atoms were placed in calculated positions and refined using a riding model.

The asymmetric unit of **6** contains one complex molecule lying on a general position. Four of the five *tert*-butyl groups in the molecule were found to be disordered during refinement, and were modeled over orientations labeled ′A′ and ′B′: C(8)–C(11) and C(26)–C(29), which were disordered in a 0.50:0.50 occupancy ratio; and C(38)–C(41) and C(50)–C(53), which were modeled with an occupancy ratio of 0.60:0.40. All disordered C–C distances were restrained to 1.52(2) Å, and non-bonded 1,3-C···C distances within a given disorder orientation to 2.48(2) Å. All non-H atoms with occupancy = 0.5 were refined anisotropically, while all H atoms were placed in calculated positions and refined by using a riding model.

Acknowledgement

The authors thank Dr. H. J. Blythe (University of Sheffield, UK) for the magnetic susceptibility data for **3**, and Mr. J. Friend (University of Manchester, UK) for help with the EPR measurements. The ES and MALDI mass spectra were obtained at the EPSRC National Mass Spectrometry facility at the University of Swansea, UK. Funding by the Royal Society of London (M.A.H.), the EPSRC (X.L., J.A.M.) and the University of Leeds is gratefully acknowledged.

[1] A. Müller, H. Reuter, S. Dillinger, *Angew. Chem.* **1995**, *107*, 2505–2539; *Angew. Chem. Int. Ed.* Engl. **1995**, *34*, 2328–2361.
[2] S. Leininger, B. Olenyuk, P. J. Stang, *Chem. Rev.* **2000**, *100*, 853–908.
[3] B. Hasenkopf, J-M. Lehn, B. O. Kneisel, G. Baum, D. Fenske, *Angew. Chem.* **1996**, *108*, 1987–1990; *Angew. Chem. Int. Ed. Engl.* **1996**, *35*, 1838–1840.
[4] a) J. S. Fleming, K. L. V. Mann, C.-A. Carraz, E. Psillakis, J. C. Jeffrey, J. A. McCleverty, M. D. Ward, *Angew. Chem.* **1998**, *110*, 1315–1318; *Angew. Chem. Int. Ed.* **1998**, *37*, 1279–1281; b) R. L. Paul, Z. R. Ball, J. C. Jeffrey, J. A. McCleverty, M. D. Ward, *Proc. Natl. Acad. Sci. USA* **2002**, *99*, 4883–4888.
[5] a) M. Scherer, D. L. Caulder, D. W. Johnson, K. N. Raymond, *Angew. Chem.* **1999**, *111*, 1690–1694; *Angew. Chem. Int. Ed.* **1999**, *38*, 1588–1592; b) M. Ziegler, A. V. Davis, D. W. Johnson, K. N. Raymond, *Angew. Chem.* **2003**, *115*, 689–692; *Angew. Chem. Int. Ed.* **2003**, *42*, 665–668.
[6] Y. Bretonnière, M. Mazzanti, J. Pécault, M. M. Olmstead, *J. Am. Chem. Soc.* **2002**, *124*, 9012–9013.
[7] X. Liu, J. A. McAllister, M. P. de Miranda, B. J. Whitaker, C. A. Kilner, M. A. Halcrow, *Angew. Chem.* **2002**, *114*, 782–784; *Angew. Chem. Int. Ed.* **2002**, *41*, 756–758.
[8] a) M. L. Ziegler, J. Weiss, *Angew. Chem.* **1970**, *82*, 931–932; *Angew. Chem. Int. Ed. Engl.* **1970**, *9*, 905–906; b) M. Ishimori, T. Hagiwara, T. Tsuruta, Y. Kai, N. Yasuoka, N. Kasai, *Bull. Chem. Soc. Jpn.* **1976**, *49*, 1165–1166.
[9] M. Shibahara, T. Yamamoto, H. Kanadani, H. Kuroya, *J. Am. Chem. Soc.* **1987**, *109*, 3495–3496.
[10] M. D. Clerk, M. J. Zaworotko, *J. Chem. Soc. Chem. Commun.* **1991**, 1607–1608.
[11] I. Büsching, H. Strasdeit, *J. Chem. Soc. Chem. Commun.* **1994**, 2789–2790.
[12] J. A. Real, G. De Munno, R. Chiapetta, M. Julve, F. Lloret, Y. Journeaux, J.-C. Colin, G. Blondin, *Angew. Chem.* **1994**, *106*, 1223–1226; *Angew. Chem. Int. Ed. Engl.* **1994**, *33*, 1184–1186.
[13] W. A. Herrmann, A. Egli, E. Herdtweck, R. Alberto, F. Baumgärtner, *Angew. Chem.* **1996**, *108*, 486–489; *Angew. Chem. Int. Ed. Engl.* **1996**, *35*, 432–434.
[14] V. Tangoulis, C. P. Raptopoulou, S. Paschalidou, E. G. Bakalbassis, S. P. Perlepes, A. Terzis, *Angew. Chem.* **1997**, *109*, 1165–1167; *Angew. Chem. Int. Ed. Engl.* **1997**, *36*, 1083–1085.
[15] K. M. Fromm, *Chem. Commun.* **1999**, 1659–1660.
[16] a) F. Benevelli, E. L. Doyle, E. A. Harron, N. Feeder, E. A. Quadrelli, D. Sáez, D. S. Wright, *Angew. Chem.* **2000**, *112*, 1561–1563; *Angew. Chem. Int. Ed.* **2000**, *39*, 1501–1503; b) D. R. Armstrong, F. Benevelli, A. D. Bond, N. Feeder, E. A. Harron, A. D. Hopkins, M. McPartlin, D. Montcrieff, D. Sáez, E. A. Quadrelli, A. D. Woods, D. S. Wright, *Inorg. Chem.* **2002**, *41*, 1492–1501.
[17] R.-K. Chiang, C.-C. Huang, C.-S. Wur, *Inorg. Chem.* **2001**, *40*, 3237–3239.
[18] S. Triki, F. Thétiot, J. S. Pala, S. Golhen, J. M. Clemente-Juan, C. J. Gómez-García, E. Coronado, *Chem. Commun.* **2001**, 2172–2173.
[19] X. Xu, S. , Gou, W. Huang, Y. Ma, Y. Li, *Eur. J. Inorg. Chem.* **2003**, 2054–2057.
[20] X. Liu, C. A. Kilner, M. Thornton-Pett, M. A. Halcrow, *Acta Crystallogr. Sect. C* **2001**, *57*, 1253–1255.
[21] M. A. Halcrow, *Dalton Trans.* **2003**, 4375–4384, and references therein.
[22] J. D. Dunitz, V. Schomaker, K. N. Trueblood, *J. Phys. Chem.* **1988**, *92*, 856–867.
[23] G. Aromi, S. Bhaduri, P. Artús, K. Folting, G. Christou, *Inorg. Chem.* **2002**, *41*, 805–817.
[24] a) D. D. Heinrich, K. Folting, W. E. Streib, J. C. Huffman, G. Christou, *J. Chem. Soc. Chem. Commun.* **1989**, 1411–1413; b) G. B. Karet, Z. Sun, D. D. Heinrich, J. K. McCusker, K. Folting, W. E. Streib, J. C. Huffman, D. N. Hendrickson, G. Christou, *Inorg. Chem.* **1996**, *35*, 6450–6460.
[25] S. Arrowsmith, M. F. A. Dove, N. Logan, M. Y. Antipin, *J. Chem. Soc. Chem. Commun.* **1995**, 627.
[26] D. Wulff-Molder, M. Meisel, *Acta Crystallogr. Sect. C* **2000**, *56*, 33–34.
[27] A. A. Zin, C. B. Knobler, D. E. Harwell, M. F. Hawthorne, *Inorg. Chem.* **1999**, *38*, 2227–2230.
[28] X. Liu, A. C. McLaughlin, M. P. de Miranda, E. J. L. McInnes, C. A. Kilner, M. A. Halcrow, *Chem. Commun.* **2002**, 2978–2979.
[29] The single-crystal structure of **5** shows a mononuclear, *trans*-$[Cu(NCS)_2(Hpz^{rBu})_2]$ molecule with an almost perfect square D_{2d}-symmetric geometry. Individual molecules are arranged into one-dimensional stacks by intermolecular N–H···S hydrogen bonding. Full details of this structure are given in the Experimental Section.
[30] G. La Monica, G. A. Ardizzoia, *Prog. Inorg. Chem.* **1997**, *46*, 151–238.
[31] a) G. B. Deacon, E. E. Delbridge, C. M. Forsyth, *Angew. Chem.* **1999**, *111*, 1880–1882; *Angew. Chem. Int. Ed.* **1999**, *38*, 1766–1767; b) A. Steiner, G. T. Lawson, B. Walfort, D. Leusser, D. Stalke, *J. Chem. Soc. Dalton Trans.* **2001**, 219–221; c) Z. Hu, S. M. Gorun, *Inorg. Chem.* **2001**, *40*, 667–671; d) J. C. Röder, F. Meyer, E. Kaifer *Angew. Chem.* **2002**, *114*, 2414–2417; *Angew. Chem. Int. Ed.* **2002**, *41*, 2304–2306.
[32] C. Mealli, C. S. Arcus, J. L. Wilkinson, T. J. Marks, J. A. Ibers, *J. Am. Chem. Soc.* **1976**, *98*, 711–718.
[33] a) C. Yelamos, M. J. Heeg, C. H. Winter, *Inorg. Chem.* **1998**, *37*, 3892–3894; b) G .B. Deacon, E. E. Delbridge, C. M. Forsyth, B. W. Skelton, A. H. White, *J. Chem. Soc. Dalton Trans.* **2000**, 745–751.
[34] G. W. Rabe, H. Heise, G. P. A. Yap, L. M. Liable-Sands, I. A. Guzei, A. L. Rheingold, *Inorg. Chem.* **1998**, *37*, 4235–4245.
[35] C. J. O′Connor, *Prog. Inorg. Chem.* **1982**, *29*, 203–283.
[36] L. Merz, W. Haase, *J. Chem. Soc. Dalton Trans.* **1980**, 875–879.

[37] V. H. Crawford, H. W. Richardson, J. R. Wasson, D. J. Hodgson, W. H. Hatfield, *Inorg. Chem.* **1976**, *15*, 2107–2110.
[38] A. Bencini, D. Gatteschi, *EPR of exchange coupled systems*, Springer, Berlin, **1990**.
[39] a) D. R. McMillin, R. S. Drago, J. A. Nusz, *J. Am. Chem. Soc.* **1976**, *98*, 3120–3126, references therein; b) Y. Sasaki, M. Sakurada, M. Matsui, T. Shigematsu, *Bull. Chem. Soc. Jpn.* **1979**, *52*, 2295–2298; c) R. Lahiri, G. N. Rao, *Thermochim. Acta* **1985**, *90*, 53–59; d) I. R. Young, L. A. Ochrymowycz, D. B. Rorabacher, *Inorg. Chem.* **1986**, *25*, 2576–2582.
[40] A. G. Orpen, L. Brammer, F. H. Allen, O. Kennard, D. G. Watson, R. Taylor, *J. Chem. Soc. Dalton Trans.* **1989**, *S1*-S83.
[41] J. C. Mareque Rivas, R. T. M. de Rosales, S. Parsons, *Dalton Trans.* **2003**, 2156–2163.
[42] J. Sletten, A. Sørensen, M. Julve, Y. Journaux, *Inorg. Chem.* **1990**, *29*, 5054–5058.
[43] a) M. Zheng, S. V. Khangulov, G. C. Dismukes, V. V. Barynin, *Inorg. Chem.* **1994**, *33*, 382–387; b) J. M. Peloquin, K. A. Campbell, D. W. Randall, M. A. Evanchik, V. L. Pecoraro, W. H. Armstrong, R. D. Britt, *J. Am. Chem. Soc.* **2000**, *122*, 10926–10942.
[44] B. Cage, F. A. Cotton, N. S. Dalal, E. A. Hillard, B. Rakvin, C. M. Ramsey, *J. Am. Chem. Soc.* **2003**, *125*, 5270–5271.
[45] F. E. Mabbs, D. Collison, *Electron Paramagnetic Resonance of d Transition Metal Compounds*, Elsevier, Amsterdam, **1992**, ch. 7.
[46] MAPLE 8, Program for the evaluation of symbolic algebra, Waterloo Maple Inc., Waterloo, Canada, **2002**.
[47] S. Fritzsche, T. Inghoff, T. Bastug, M. Tomaselli, *Comput. Phys. Commun.* **2001**, *139*, 314–326.
[48] W. H. Press, S. A. Teukolsky, W. T. Vetterling, B. P. Flannery, *Numerical Recipes: the Art of Scientific Computing*, Cambridge University Press, Cambridge, UK, **1992**.
[49] S. Trofimenko, J. C. Calabrese, J. S. Thompson, *Inorg. Chem.* **1987**, *26*, 1507–1514.
[50] G. M. Sheldrick, SHELXS 97, Program for the solution of crystal structures, University of Göttingen, Germany, **1997**.
[51] G. M. Sheldrick, *Acta Crystallogr. Sect. A* **1990**, *46*, 467–473.
[52] Sheldrick, SHELXL 97, Program for the refinement of crystal structures, University of Göttingen, Germany, **1997**.
[53] A. L. Spek, *PLATON, A multipurpose crystallographic tool*, Utrecht University, Utrecht, Netherlands, **2003**.

Received: October 10, 2003
Revised: January 13, 2004 [F5613]

